Wall-less Flow Phantom for High-Frequency Ultrasound Applications

Ultrasound in Med. & Biol., Vol. ■, No. ■, pp. 1–8, 2014

0301-5629/$ - see front matter

http://dx.doi.org/10.1016/j.ultrasmedbio.2014.09.018

● *Technical Note*

WALL-LESS FLOW PHANTOM FOR HIGH-FREQUENCY ULTRASOUND APPLICATIONS

David A. Kenwright, Nicola Laverick, Tom Anderson, Carmel M. Moran, and Peter R. Hoskins

Centre for Cardiovascular Science, University of Edinburgh, Edinburgh, United Kingdom

(*Received* 4 *August* 2014; *revised* 10 *September* 2014; *in final form* 11 *September* 2014)

Abstract—There are currently very few test objects suitable for high-frequency ultrasound scanners that can be rapidly manufactured, have appropriate acoustic characteristics and are suitably robust. Here we describe techniques for the creation of a wall-less flow phantom using a physically robust konjac and carrageenan-based tissue-mimicking material. Vessel dimensions equivalent to those of mouse and rat arteries were achieved with steady flow, with the vessel at a depth of 1.0 mm. We then employed the phantom to briefly investigate velocity errors using pulsed wave Doppler with a commercial preclinical ultrasound system. This phantom will provide a useful tool for testing preclinical ultrasound imaging systems. (E-mail: david.kenwright@ed.ac.uk) **© 2014 World Federation for Ultrasound in Medicine & Biology.**

Key Words: **Ultrasound, High frequency, Tissue-mimicking material, Preclinical ultrasound, Wall-less flow phantom.**

INTRODUCTION

Ultrasound provides a method of measuring blood flow, with applications including: estimation of the degree of stenosis (narrowing of vessels) for selection of patients for carotid surgery (Grant et al. 2003); measurement of the downstream resistance to flow, as estimated from the pulsatility index (Chen et al. 1993); measurement of blood velocity as a surrogate for volumetric blood flow (Bishop et al. 1986; Doucette et al. 1992); and measurement of wall shear stress as a predictor of atherogenic risk (Blake et al. 2008; Brands et al. 1995; Kornet et al. 1998). As such, the ability to accurately measure the velocity of blood flow in vessels is of great importance in clinical practice and research studies. Flow phantoms that simulate these conditions are vital for the accurate determination of these quantities, for assessment of the performance of equipment and for investigation of the reproducibility of parameters required for the evaluation of new methodologies.

Address correspondence to: David A. Kenwright, Centre for Cardiovascular Science, University of Edinburgh, The Queen's Medical Research Institute, 47 Little France Crescent, Edinburgh EH16 4 TJ, UK. E-mail: david.kenwright@ed.ac.uk

This work was supported by British Heart Foundation Project Grant PG/10/012/28201.

Flow phantoms provide a controllable experimental system against which hypotheses can be tested or measurements validated and, as such, should be relevant to the subject under examination. Flow phantoms for clinical ultrasound systems first appeared more than 40 y ago (Michie and Fried 1973). A review of steady flow systems appeared in Law et al. (1989), after which attempts were made to develop phantoms using materials that more closely matched the ultrasonic properties of tissue (reviewed in Hoskins 2008). Tissue-mimicking materials (TMMs) with a speed of sound and acoustic attenuation equivalent to values in human soft tissue were investigated, and the International Electrotechnical Commission (IEC) (2001) specified the required parameters and values. With the advent of commercial high-frequency ultrasound systems specifically designed for imaging small animals (Foster et al. 2002, 2009), test objects have been adapted to suit these applications (Madsen et al. 2010; Moran et al. 2011; Yang et al. 2013).

A flow phantom will typically consist of a vessel suspended in TMM, designed to have the same acoustic properties as soft tissue. A blood-mimicking fluid (BMF), with acoustic properties matching those of blood, is pumped through the phantom. For clinical and, therefore, low-frequency applications, the vessel may be a

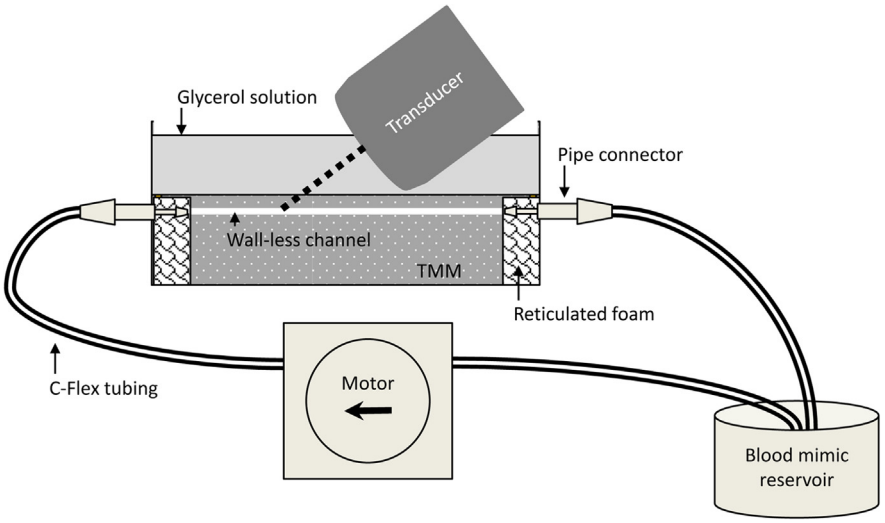

Fig. 1. Schematic diagram of the flow phantom illustrating acquisition of Doppler measurements. TMM = tissue-mimicking material.

rubber-based material (such as latex rubber or C-Flex tubing) or a polyvinyl alcohol–cryogel (Dineley et al. 2006). For more complex geometries, a wall-less approach has been adopted (Meagher et al. 2007; Ramnarine et al. 2001).

An important consideration in flow phantom design is that the vessel should be similar in size and positioned at a depth similar to those of the vessel under consideration *in vivo*. In preclinical research, which uses animals such as mice and rats to develop new diagnostic techniques and treatments before clinical trials on humans, the structures being studied are generally much smaller than those in humans. Therefore preclinical ultrasound scanners must operate at higher frequencies to provide the necessary resolution, typically in the region 20–50 MHz (Foster et al. 2002, 2009). As this increase in frequency reduces the penetration depth, flow phantom design must take this into consideration. A flow phantom with vessel diameters of 1 mm was briefly described in Foster et al. (2009), who used a gelatin-based vessel-mimicking material with a gravity-fed flow of de-ionized water containing a dilute solution of microbubble contrast. Phantoms that mimic the human microcirculation have also been developed, where the vessel dimensions are similar in size to those of mouse and rat arteries, although designed for much lower rates of flow to replicate perfusion at the capillary bed (Eriksson et al. 1995; Pinter and Lacefield 2009; Veltmann et al. 2002).

Here we describe a wall-less flow phantom suitable for use in the assessment of high-frequency ultrasound scanners using materials suitable for high-frequency ultrasound applications.

METHODS

Initial design

In initial designs of the phantom, C-Flex tubing (Cole–Parmer, Niles, IL, USA) was used to create a vessel embedded in agar-based TMM (Teirlinck et al. 1998). However, because of the attenuation of the ultrasound signal through the C-Flex, a spectral Doppler trace from the blood mimic could not be obtained. Next a wall-less design based on a reduced-scale version of the phantom described in Ramnarine et al. (2001) was used. However, it was found that the agar-based TMM ruptured immediately after flow was started because of the shallow depth of the vessel. Therefore, an alternative TMM was required for the wall-less design. A TMM based on the hydrogels konjac and carrageenan was used in this study as a stronger alternative (Meagher et al. 2007). This TMM has recently been acoustically characterized in the frequency range 5–60 MHz and is, therefore, suitable for use in preclinical ultrasound phantoms (Kenwright et al. 2014).

Phantom construction

Figure 1 illustrates the phantom and measurement setup. A sealable plastic box acted as the container for the phantom. Holes were drilled in two sides, and reducing pipe connectors (Cole–Parmer) were glued in place with Araldite Rapid (Huntsman Advanced Materials, Basel, Switzerland). Reticulated foam (pore size 1–2 mm) was glued with Araldite to the inside wall and around the pipe connectors in the box. The reticulated foam provided a fixed structure into which the TMM could flow when molten and, once set, prevented the TMM from coming away from the connectors and the

Table 1. Composition of the konjac–carrageenan tissue-mimicking material

Component	Manufacturer	Weight (%)
De-ionized water		84
Glycerol	Sigma–Aldrich, Dorset, UK	10
Silicon carbide 400 grain	Logitech, Glasgow, UK	0.53
Aluminum powder (3 μm)	Logitech	0.96
Aluminum powder (0.3 μm)	Logitech	0.89
Konjac powder	FMC Biopolymer, Philadelphia, PA, USA	1.5
Carrageenan powder	Sigma–Aldrich	1.5
Potassium chloride	Sigma–Aldrich	0.7

box when flow was applied. A metal rod acted as the mold for the vessel, with diameters between 1 and 2 mm, typical of rat femoral and common carotid arteries (Nam et al. 2014; Rickard et al. 2009). The rod was inserted through both of the pipe connectors, which were aligned to ensure that the rod was straight.

Here we provide a detailed guide to producing the konjac–carrageenan TMM (for full composition, see Table 1). The metal particles (0.3- and 3-μm aluminum oxide and silicon carbide) were weighed in turn, mixed in a beaker until uniform and then sieved into the required quantity of de-ionized water. A whisk was used to mix the particles and to further break up any clumps. The mixture was then degassed in a vacuum chamber at 4.8 MPa; if the bubbles threatened to overflow the container, the pressure was briefly released. This was repeated until no further bubbles formed in the mixture. The container was then placed in a water bath, and the mixture stirred with an electric mixer at approximately two rotations per second. This rate ensured that the particles did not settle, while being sufficiently slow to not promote air bubbles. The water bath heater was set to 90°C; when the bath temperature reached 60°C, the konjac and carrageenan powders were mixed together and sieved into the water/metal particle mixture while the mixture continued to be heated and stirred. The powders were added slowly to allow them to mix into the water without forming clumps.

Once the water bath had reached 90°C, the mixture was left to heat at this temperature under continuous stirring for 1 h. At the end of this period, the gel had melted and was homogenous. The glycerol was then added and mixed for a further 10 min. After this, the heater was switched off, and the TMM was left to cool while still being stirred until the water bath temperature reached 80°C.

The TMM was then poured into the phantom mold, covering the metal rod by approximately 1.0 mm. This depth was used to provide sufficient covering to form a strong upper vessel wall while being sufficiently shallow to allow the transducer to come close enough to obtain images from a variety of angles. The TMM was left to cool and then covered with a 9% glycerol solution with a speed of sound of 1540 m s^{-1}, enabling coupling of the ultrasound from the probe and also preventing the TMM from drying out.

The rods were removed, and C-flex tubing (Cole–Parmer) was then attached to the external ends of the connectors to act as feed-in and feed-out pipes.

Blood-mimicking fluid preparation

The blood mimic consisted of a suspension of 5-μm nylon particles in a glycerol/dextran solution with blood-equivalent acoustic and viscous properties (Ramnarine et al. 1998; Ramnarine and Hoskins 1999). Because of the high sensitivity of high-frequency ultrasound scanners, the BMF was circulated through a large gear pump (GJ-N2, Micropump, Vancouver, WA, USA) for approximately 5 h, to break up any clumping of the powders, and degassed for approximately 3 h before use. This removes spikes in the Doppler trace caused by high reflections from clumps of the particles and bubbles in the BMF (Fig. 2). For use with the phantom, the BMF was circulated using a smaller gear pump (GA-v21, Micropump) at a steady flow rate equivalent to a mean velocity between 10 and 35 cm s^{-1}.

Ultrasound data acquisition

A Vevo 770 preclinical ultrasound scanner (FUJIFILM VisualSonics, Toronto, ON, Canada; equipped with four different transducers with central frequencies ranging from 20 to 40 MHz) was used to collect ultrasound data from the phantom. The transducers were held in an adjustable transducer stand, and the phantom on a bench-mounted adjustable rail system. The transducers were fixed at a desired angle and lowered as close as possible to the surface of the phantom without pressing into the TMM. As the vessel is a long, straight tube, the direction of flow (and, therefore, the mean area velocity) of the BMF will be in line with the vessel axis, parallel to the vessel wall. The angle cursor of the on-board software was aligned with the direction of flow (all angle measurements are $\pm 0.5°$ as the cursor step in the software is 1°). This determines the angle between the ultrasound beam and the direction of flow, as used in the Doppler equation. The maximum velocity of the BMF was measured with the Vevo 770 operating in pulsed wave (PW) Doppler mode. The gate length was set so that the entire vessel was within the gate. With steady flow applied, the maximum velocity (V_{max}) was measured by taking the average (over approximately 1 s) maximum trace of the PW Doppler signal using the Vevo 770 on-board software.

Vessel diameter was the average of three measurements determined in B-mode with the transducer

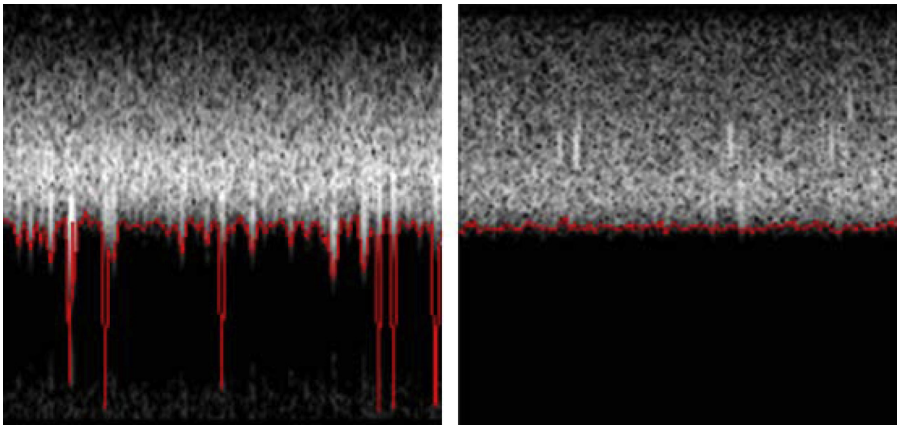

Fig. 2. Doppler trace of the BMF after being made with the standard procedure (left) and after processing through a gear pump before degassing (right). This process removes the spikes in the Doppler trace caused by air and clumps of particles and enables more accurate velocity estimation, as can be seen from the automated trace of the maximum velocity (*red lines*). BMF = blood-mimicking fluid.

perpendicular to the vessel. Because of the deformability of the TMM, there was a change in vessel diameter when the flow was applied. For example, a vessel with a diameter of 1.42 ± 0.01 mm would increase to a diameter of 1.47 ± 0.01 mm when a flow rate of 32 ± 1 cm s^{-1} was applied. The flow rate in milliliters per minute through the circuit was measured with a graduated cylinder and a stopwatch. The cross-sectional area of the vessel was calculated using the diameter measurements with flow applied. These values were then used to estimate the true mean velocity of the BMF through the phantom using the relationship flow = velocity × area. Assuming parabolic flow, the mean velocity is half of the maximum velocity (as measured from the Doppler spectra).

Verifying parabolic flow

To ensure fully established laminar flow profiles, the inlet length (L) must be at least

$$L = 0.04 \times D \times \mathrm{Re} \tag{1}$$

(McDonald 1974), where D is the diameter of the vessel, and Re is the Reynolds number, given by

$$\mathrm{Re} = \frac{\rho v D}{\mu}, \tag{2}$$

where ρ is the density of the BMF (1.037 kg cm^{-3} [Ramnarine et al. 1998]), v is the mean velocity and μ is the viscosity (4.1 mPa·s). The minimum entrance length for BMF traveling at 20 cm s^{-1} through a diameter of 1.5 mm is 0.44 mm. Measurements were carried out sufficiently far from the inlet of the phantom (>1 cm) to ensure that fully developed flow was achieved at the measurement site. The verification was carried out using a 1.47 ± 0.01-mm-diameter vessel and the RMV710B transducer. The probe was held at a fixed angle to the vessel, the minimum gate length was selected (0.08 mm) and a maximum velocity measurement was made. The gate was moved vertically downward along the acoustic beam, and measurements were taken at multiple depths. The depth measurements were corrected so that the velocities were associated with various depths across the vessel. The correct depth D_{corr} was calculated as

$$D_{corr} = (D - D_0) \sin\theta, \tag{3}$$

where D is the vertical measurement, D_0 is the vertical depth of the upper edge of the vessel and θ is the angle between the vessel and the ultrasound beam.

Velocity error calculation

For parabolic flow, the mean velocity is half of the maximum velocity; therefore the mean velocity as determined by ultrasound ($V_{ultrasound}$) = $V_{max}/2$. Velocity measurements were taken for a variety of angles for each transducer. The true mean velocity (V_{true}) across the cross-sectional area of the BMF was measured by timed collection, as described above. The percentage velocity error for each angle was calculated as

$$\%\mathrm{Error} = 100 \times \frac{V_{ultrasound} - V_{true}}{V_{true}}. \tag{4}$$

The percentage error could then be plotted against beam target angle. This procedure was followed to collect data using the four available transducers (for details on the center frequencies and focal lengths of the transducers, see Table 2).

Table 2. Center frequency, focal depth and minimum measured Doppler angle for each of the VisualSonics transducers

Transducer model	Center frequency (MHz)	Focal depth (mm)	Minimum measurement angle
RMV704	30	6	63°
RMV707B	23	12.7	49°
RMV710B	20	15	43°
RMV711	40	6	54°

RESULTS

In Figure 3 are a typical B-mode image and PW Doppler spectra from a vessel with an inner diameter of 1.47 mm when flow is applied, comparable in size to a rat common carotid artery. The maximum velocity was obtained from a time average using the on-board software on the Vevo 770.

Velocity profile

The velocity profile obtained from a phantom with a vessel diameter of 1.47 mm appears in Figure 4. Measurements were taken using the RMV710 probe, with the ultrasound beam at an angle of 63° to the vessel wall. The peak velocity is located at the center of the vessel, decreasing to a minimum at the vessel walls. Figure 4 illustrates that a parabola is a good fit to the data in the form $aD^2 + bD + c$ with an R^2 of 0.95, where a, b and c are constants, and D is the depth of measurement along the vessel diameter; therefore, the flow can be considered fully developed.

Doppler angle

The range of angles from which reliable Doppler signals could be obtained was 43°–79° (79° being the maximum allowed by the Vevo 770). The minimum angles obtained for each transducer are listed in Table 2.

Figure 5 illustrates the velocity error in the measurements with changing angle between the ultrasound beam and the direction of flow, as determined by the angle cursor in the Vevo 770 on-board software. The error in velocity increased with increasing Doppler angle, ranging from 15%–95%.

DISCUSSION

In this article, we have described the manufacture and use of a wall-less flow phantom suitable for comparison to preclinical ultrasound studies. Usually a vessel of small depth is required to enable Doppler measurements to be reliably performed. A phantom with a small vessel depth would usually require a vessel wall to prevent rupture (Hoskins et al. 2010); however, this has the disadvantage of potential impedance mismatches at the boundaries, which will cause refraction. Although there are vessel-mimicking materials with a speed of sound similar to that of tissue, such as the IEC-recommended C-Flex tubing (IEC 2001), the attenuation of this is approximately 10 times higher than that of soft tissue (Hoskins 2008), which prevents the ultrasonic beam from penetrating to a sufficient depth to obtain a Doppler signal with the transducers under investigation. For wall-less approaches, the small depth of the vessel can be a limiting factor because of rupture. Because of the robust nature of the TMM used in this study, a wall-less approach was taken with as little as 1.0 mm of TMM on the upper surface, comparable to the depth of a rat femoral artery. This, therefore, removes the attenuation problem and minimizes errors associated with impedance mismatches of different materials.

The flow profile of BMF through the phantom fits a parabola, and therefore, we can be confident that the flow is laminar (Evans and McDicken 2000). This is an important consideration in flow phantom design, as a value for the "true" maximum velocity is estimated from timed volume collection with an assumption of parabolic flow, where the maximum velocity is equal to twice the mean velocity.

The angles over which reliable Doppler measurements could be taken ranged between 43°–79°, the upper value being the maximum allowed by the scanner. The lower value varied between transducers because of a combination of the focal depth and the width of the casing surrounding the transducer. Care had to be taken to ensure that the transducer did not press into the TMM, which would have had the effect of narrowing the vessel diameter as the TMM deformed, which is more problematic for the larger transducers. For example, although the 704 and 711 transducers have the same focal depth (6 mm), the profile of the 711 is narrower than that of the 704, allowing a shallower angle to be obtained. This range of angles is an important consideration if a phantom is used to compare measurements taken at multiple angles and to account for effects such as geometric spectral broadening. The experience in our institution is that Doppler angles for the carotid and femoral arteries in rats are typically greater than 45°, at which errors in velocity estimation can be as high as 30% (Yang et al. 2013). By use of a linear array system, the Doppler beam can be steered and a greater range of angles can be obtained from multiple focal depths.

The increase in velocity error with measurement angle observed with the wall-less phantom is consistent with geometric spectral broadening. This is the effect whereby the transducer used to transmit and receive the Doppler beam is of finite width, meaning that the target velocity vector subtends a range of angles at the Doppler aperture and causes a spread in frequency of the received

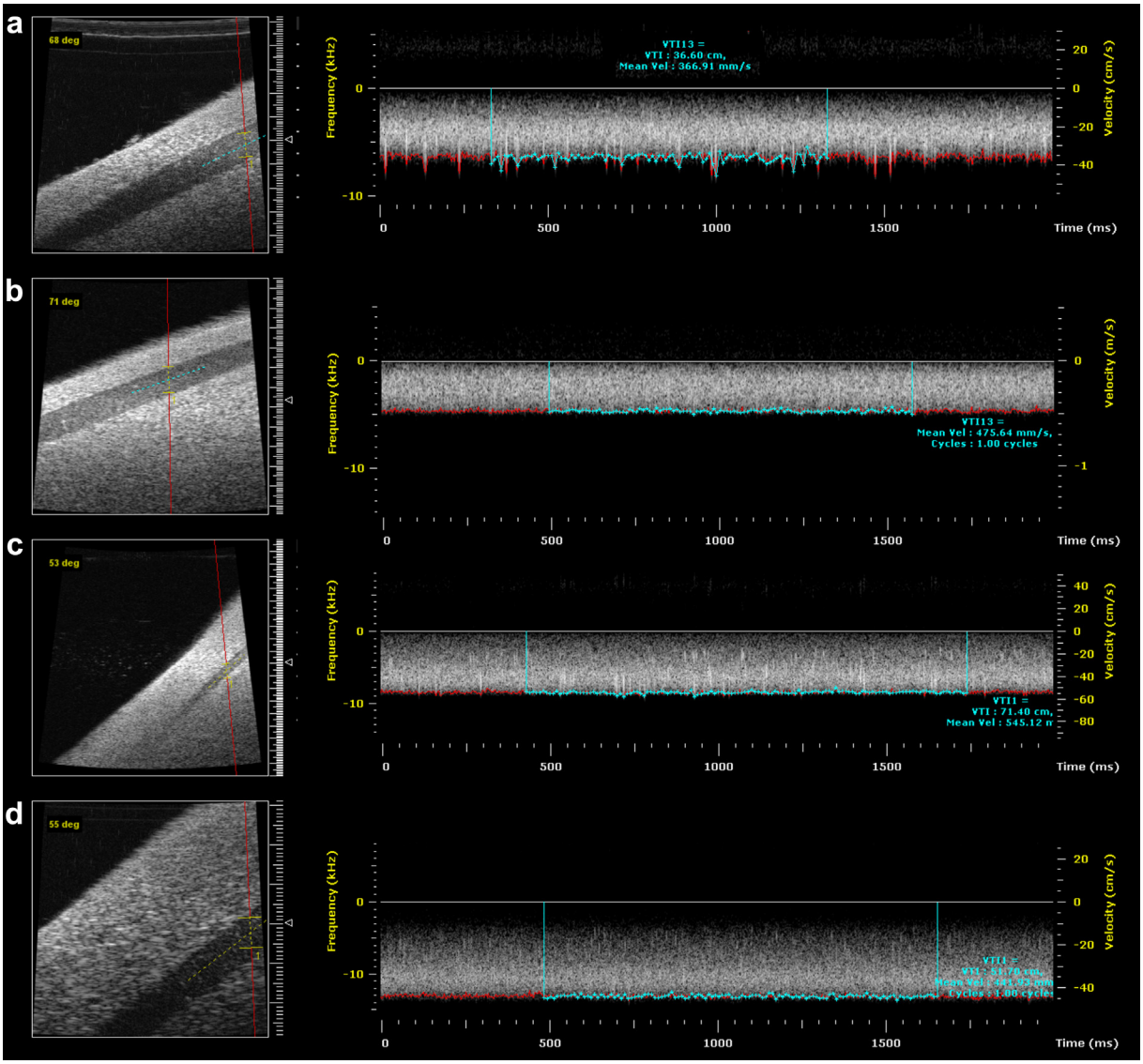

Fig. 3. B-Mode (left) and pulsed wave Doppler spectrum (right) images of (a) a 1.00-mm-diameter phantom, with the RMV704 transducer operating at 30 MHz; (b) a 1.47-mm-diameter phantom, with the RMV707B transducer operating at 23 MHz; (c) a 1.00-mm-diameter phantom, with the RMV710B transducer operating at 20 MHz; and (d) a 1.00-mm-diameter phantom, with the RMV711 transducer operating at 40 MHz obtained using the Vevo 770 ultrasound system. The B-mode images show the vessel oriented at an angle to the ultrasonic beam (*red line*), with the sample volume indicated by the yellow callipers. The pulsed wave Doppler spectra reveal the frequency shift of the ultrasound beam within the sample volume. The velocity of the blood-mimicking fluid is determined from the automated peak-frequency trace (*red line*) averaged over a selected section (*yellow line*). In example (b), the measured velocity from pulsed wave Doppler is 47.6 cm s^{-1}, whereas the true maximum velocity is 33 ± 1 cm s^{-1}, as determined by timed collection.

signal (Hoskins 1999). This has previously been investigated for the Vevo 770 using a rotating phantom (Yang et al. 2013). A detailed investigation of velocity errors using different transducers is outside the scope of this article.

The vessel diameter of the phantom changed when flow was applied. It is important that for the correct calculation of flow values from velocity measurements, the diameter should be measured when flow is applied to avoid an overestimation of flow rate.

In addition to the original methodology described for creating the BMF (Ramnarine et al. 1998), we found it necessary to run the BMF through a gear pump for several hours for use with a preclinical ultrasound scanner before degassing in a vacuum chamber. This increases the preparation time from approximately 3–4 to 8–9 h, but prevents clumping in the suspension of particles which can cause high-reflection spikes in the Doppler signal that would affect the velocity estimation. It should also

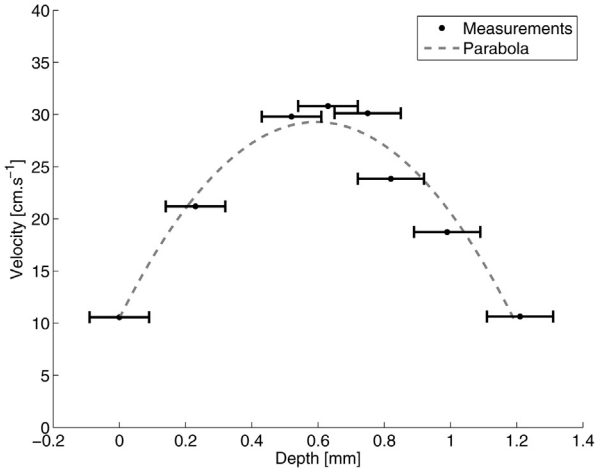

Fig. 4. Velocity profile of blood-mimicking fluid in a 1.47-mm phantom obtained using the RMV710 transducer operating at 20 MHz. The *dashed line* is a parabolic fit to the data in the form aD^2+bD+c with an R^2 of 0.95, where a, b and c are constants, and D is the depth of measurement from the vessel wall. As the flow is approximately parabolic, we can therefore use the maximum velocity (V_{max}) to estimate the mean velocity as $V_{max}/2$.

be noted that the BMF should not be allowed to remain in the phantom when not in use, as settling of the particles can occur, blocking the vessel or narrowing the effective diameter in future use. A matched glycerol solution should be pumped through the vessel between uses to remove the BMF and to prevent changes in the TMM composition over time. If the BMF is to be re-used, it should be passed through the larger gear pump and degassed again before use.

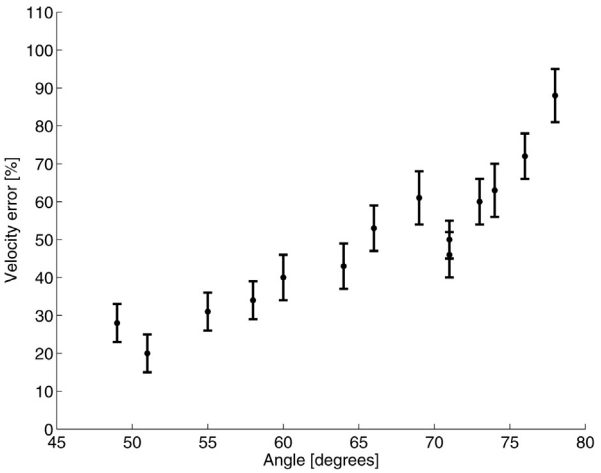

Fig. 5. Percentage difference in the measured maximum velocity from the true velocity of the blood-mimicking fluid in the phantom as a function of beam–target angle using a Vevo770 ultrasound system with a RMV707B transducer operating at 23 MHz and 1.47-mm-diameter flow phantom. Despite correct adjustment of the Doppler angle cursor, there is an increasing difference between the true velocity and the measured velocity with beam angle.

Blood flow *in vivo* is generally pulsatile in nature, rather than steady. It would be possible to adapt the phantom described in this article for pulsatile flow by attaching a computer-controlled waveform generator to the pump power supply (*e.g.*, Ramnarine et al. 2001). The mean flow (and, thus, the peak velocity) of the blood mimic may need to be reduced to prevent rupture at higher velocities. Further characterization of the TMM would be required to ensure that the elastic properties are appropriate to achieve biologically equivalent diameter changes during each pulse cycle. Although pulsatile flow is a more realistic model of arterial flow, the resultant complexity of the flow field and velocity profile make the interpretation of the Doppler signal more difficult. Therefore, steady flow can be advantageous where laminar flow is required, such as in evaluating velocity errors in Doppler signals.

Although we have dealt with an ideal case of a long, straight vessel, it is true that arteries *in vivo* are rarely so. The wall-less design of the phantom also allows for the potential to create more complex geometries, such as stenosis (Ramnarine et al. 2001) or artery bifurcations (Meagher et al. 2007). This provides scope for future investigations to be carried out with only minor modifications to the specifications described in this article.

CONCLUSIONS

We have described the design of a flow phantom that is suitable for comparison to preclinical investigations of Doppler ultrasound. Velocity errors were briefly investigated as a trial experiment for the phantom. The ability of the phantom to form a wall-less vessel between 1 and 1.5 mm in diameter, with only a 1.0-mm proximal thickness of TMM, ensures that probes can be brought sufficiently close to the vessel to obtain reliable Doppler measurements. The minimum achievable Doppler angle using the available Vevo 770 transducers with this phantom was 43°, similar to angles obtainable during *in vivo* experiments.

Acknowledgments—We thank Xin Yang and Kirsten Graham for preliminary work leading to this study. We are also grateful to Gillian A Gray and Patrick W Hadoke for useful comments.

REFERENCES

Bishop CCR, Powell S, Rutt D, Browse NL. Transcranial Doppler measurement of middle cerebral-artery blood-flow velocity: A validation study. Stroke 1986;17:913–915.

Blake JR, Meagher SC, Fraser KH, Easson WJ, Hoskins PR. A method to estimate wall shear rate with clinical ultrasound scanners. Ultrasound Med Biol 2008;34:760–774.

Brands PJ, Hoeks APG, Hofstra L, Reneman RS. Noninvasive method to estimate wall shear rate using ultrasound. Ultrasound Med Biol 1995;21:171–185.

Chen JH, Pu YS, Liu SP, Chiu TY. Renal hemodynamics in patients with obstructive uropathy evaluated by duplex-Doppler sonography. J Urol 1993;150:18–21.

Dineley JA, Meagher S, Poepping TL, McDicken WN, Hoskins PR. Design and characterization of a wall motion phantom. Ultrasound Med Biol 2006;32:1349–1357.

Doucette JW, Corl PD, Payne HM, Flynn AE, Goto M, Nassi M, Segal J. Validation of a Doppler guide wire for intravascular measurement of coronary-artery flow velocity. Circulation 1992;85:1899–1911.

Eriksson R, Persson HW, Dymling SO, Lindström K. A microcirculation phantom for performance testing of blood perfusion measurement equipment. Eur J Ultrasound 1995;2:65–75.

Evans DH, McDicken WN. Doppler ultrasound. 2nd ed. Chichester: Wiley; 2000.

Foster FS, Mehi J, Lukacs M, Hirson D, White C, Chaggares C, Needles A. A new 15–50 MHz array-based micro-ultrasound scanner for preclinical imaging. Ultrasound Med Biol 2009;35:1700–1708.

Foster FS, Zhang MY, Zhou YQ, Liu G, Mehi J, Cherin E, Harasiewica KA, Starkoskki BG, Zan L, Knapik DA, Adamson SL. A new ultrasound instrument for in vivo microimaging of mice. Ultrasound Med Biol 2002;28:1165–1172.

Grant EG, Benson CB, Moneta GL, Alexandrov AV, Baker JD, Bluth EI, Carroll BA, Eliasziw M, Gocke J, Hertzberg BS, Katanick S, Needleman L, Pellerito J, Polak JF, Rholl KS, Wooster DL, Zierler RE. Carotid artery stenosis: Gray-scale and Doppler US diagnosis—Society of Radiologists in Ultrasound consensus conference. Radiology 2003;229:340–346.

Hoskins PR. A comparison of single- and dual-beam methods for maximum velocity estimation. Ultrasound Med Biol 1999;25:583–592.

Hoskins PR. Simulation and validation of arterial ultrasound imaging and blood flow. Ultrasound Med Biol 2008;34:693–717.

Hoskins PR, Soldan M, Fortune S, Inglis S, Anderson T, Plevris J. Validation of endoscopic ultrasound measured flow rate in the azygos vein using a flow phantom. Ultrasound Med Biol 2010;36:1957–1964.

International Electrotechnical Commission (IEC). Ultrasonics—Flow measurement systems: Flow test object, IEC 61685. Geneva: Author; 2001.

Kenwright DA, Sadhoo N, Rajagopal S, Anderson T, Moran CM, Hadoke PW, Gray GA, Zeqiri B, Hoskins PR. Acoustic assessment of a konjac–carrageenan tissue-mimicking material at 5–60 MHz. Ultrasound Med Biol 2014;40:2595–2902.

Kornet L, Lambregts JAC, Hoeks APG, Reneman RS. Differences in near-wall shear rate in the carotid artery within patients are associated with different intima-media thicknesses. Arterioscl Thromb Vasc Biol 1998;18:1877–1884.

Law YF, Johnston KW, Routh HF, Cobbold RSC. On the design and evaluation of a steady flow model for Doppler ultrasound studies. Ultrasound Med Biol 1989;15:505–516.

Madsen EL, Frank GR, McCormick MM, Deaner ME, Stiles TA. Anechoic sphere phantoms for estimating 3-D resolution of very-high-frequency ultrasound scanners. IEEE Trans Ultrason Ferroelectr Freq Control 2010;57:2284–2292.

McDonald DA. Blood flow in arteries. London: Edward Arnold; 1974. p. 111.

Meagher S, Poepping TL, Ramnarine KV, Black RA, Hoskins PR. Anatomic flow phantoms of the nonplanar carotid bifurcation: Part II: Experimental validation with Doppler ultrasound. Ultrasound Med Biol 2007;33:303–310.

Michie DD, Fried WL. An in vitro test medium for evaluating clinical Doppler ultrasonic flow systems. J Clin Ultrasound 1973;1:130–133.

Moran CM, Pye SD, Ellis W, Janeczko A, Morris KD, McNeilly AS, Fraser HM. A comparison of the imaging performance of high resolution ultrasound scanners for preclinical imaging. Ultrasound Med Biol 2011;37:493–501.

Nam KH, Bok TH, Jin C, Paeng DG. Asymmetric radial expansion and contraction of rat carotid artery observed using a high-resolution ultrasound imaging system. Ultrasonics 2014;54:233–240.

Pinter SZ, Lacefield JC. Detectability of small blood vessels with high-frequency power Doppler and selection of wall filter cut-off velocity for micro-vascular imaging. Ultrasound Med Biol 2009;35:1217–1228.

Ramnarine KV, Anderson T, Hoskins PR. Construction and geometric stability of physiologic flow rate wall-less stenosis phantoms. Ultrasound Med Biol 2001;27:245–250.

Ramnarine KV, Hoskins PR. Doppler backscatter properties of a blood-mimicking fluid for Doppler performance assessment. Ultrasound Med Biol 1999;25:105–110.

Ramnarine KV, Nassiri DK, Hoskins PR, Lubbers J. Validation of a new blood mimicking fluid for use in Doppler flow test objects. Ultrasound Med Biol 1998;24:451–459.

Rickard RF, Wilson J, Hudson DA. Characterization of a rodent model for the study of arterial microanastomoses with size discrepancy (small-to-large). Lab Anim 2009;43:350–356.

Teirlinck CJ, Bezemer RA, Kollmann C, Lubbers J, Hoskins PR, Ramnarine KV, Fish PJ, Fredeldt KE, Schaarschmidt UG. Development of an example test object and comparison of five of these test objects, constructed in various laboratories. Ultrasonics 1998;36:653–660.

Veltmann C, Lohmaier S, Schlosser T, Shai S, Ehlgen A, Pohl C, Becher H, Tiemann K. On the design of a capillary flow phantom for the evaluation of ultrasound contrast agents at very low flow velocities. Ultrasound Med Biol 2002;28:625–634.

Yang X, Sun C, Anderson T, Moran CM, Hadoke PWF, Gray GA, Hoskins PR. Assessment of spectral Doppler in preclinical ultrasound using a small-size rotating phantom. Ultrasound Med Biol 2013;39:1491–1499.